International Journal of Advance Research in Science and Engineering
Volume No. 15, Issue No. 03, March 2026
www.ijarse.com
IJARSE
ISSN 2319 - 8354

Theoretical Simulation and Efficiency Enhancement Study of $CsSnBr_3/FASnI_3$ Based Tin-Perovskite Solar Cell Using SCAPS-1D

M. Jahan[1], N. Vrind[2], U. Prasad[3]

[1]*Research Scholar, University Department of Physics, T.M.B.U. Bhagalpur*

[2]*Research Scholar, University Department of Physics, T.M.B.U. Bhagalpur*

[3]*Retd. Associate Professor, T.N.B. College, T.M.B.U. Bhagalpur*

Abstract

In the present work, a lead-free heterojunction perovskite solar cell based on $CsSnBr_3$ and $FASnI_3$ has been numerically investigated using SCAPS-1D simulation software. The device architecture consists of SnO_2 as the electron transport layer (ETL), $CsSnBr_3$ as a wide band gap perovskite layer, $FASnI_3$ as the primary absorber layer, HTL as the hole transport layer, and Au as the back contact. Energy band alignment, electric field distribution, recombination rate profile, and J–V characteristics were systematically analyzed. The optimized device exhibits an open-circuit voltage (V_{oc}) of 0.88 V, short-circuit current density (J_{sc}) of 26.2 mA/cm², fill factor (FF) of 76.8%, and power conversion efficiency (PCE) of 17.8%. The results demonstrate that proper band alignment and reduced recombination at the heterointerface significantly enhance device performance. This study provides a promising pathway toward efficient and environmentally friendly tin-based perovskite solar cells.

Keywords: *Lead-free perovskite, $CsSnBr_3$, $FASnI_3$, SCAPS-1D, heterojunction, solar cell simulation etc.*

1. Introduction

Perovskite solar cells (PSCs) have emerged as one of the most promising photovoltaic technologies due to their outstanding optoelectronic properties and rapid progress in power conversion efficiency. Since the first report on organometal halide perovskites for photovoltaic applications by Kojima et al. [1], device efficiencies have dramatically improved, as reflected in the recent efficiency reports and photovoltaic tables [2,3]. The remarkable performance of perovskite materials arises from their high absorption coefficient, long carrier diffusion length, low exciton binding energy, and tunable direct band gap [3]. According to the Shockley–Queisser detailed balance theory, the optimal band gap for single-junction solar cells lies near 1.34–1.45 eV [4], which makes several halide perovskites highly suitable for efficient solar energy conversion.

Despite these advantages, most high-efficiency PSCs are based on lead (Pb)-containing materials, raising environmental and toxicity concerns that may limit their commercial deployment [5]. To overcome this issue, extensive research has been devoted to developing lead-free perovskite alternatives. Among the potential

10.5281/zenodo.18832813

candidates, tin (Sn)-based perovskites have gained significant attention because Sn belongs to the same group as Pb and exhibits similar electronic configuration and band structure characteristics [6]. In particular, $FASnI_3$ (formamidinium tin iodide) possesses a direct band gap of approximately 1.41 eV, which is close to the Shockley–Queisser optimum, along with strong optical absorption and favorable charge transport properties [7]. These properties make $FASnI_3$ a promising absorber material for environmentally friendly perovskite solar cells.

However, Sn-based perovskites suffer from intrinsic instability due to the facile oxidation of Sn^{2+} to Sn^{4+}, leading to high defect density, increased background carrier concentration, and severe non-radiative recombination losses [8]. Recombination mechanisms significantly influence open-circuit voltage and overall device performance, necessitating effective strategies for defect control and interface engineering [9]. One promising approach to mitigate recombination and enhance charge separation is heterojunction engineering using materials with complementary band gaps. Incorporating a wide band gap inorganic tin perovskite such as $CsSnBr_3$ ($E_g \approx 1.75$ eV) can improve band alignment and strengthen the internal electric field when combined with a narrow band gap absorber like $FASnI_3$ [10]. Proper conduction and valence band offsets at the heterointerface can facilitate efficient carrier extraction while suppressing interfacial recombination.

In this study, a lead-free heterojunction perovskite solar cell based on the $SnO_2/CsSnBr_3/FASnI_3/HTL/Au$ architecture is numerically investigated using SCAPS-1D simulation. The effects of band alignment, electric field distribution, and recombination dynamics on photovoltaic performance are systematically analyzed to explore the potential of tin-based heterostructure engineering for high-efficiency and environmentally sustainable solar cells.

2. Device Structure and Simulation Methodology

2.1. Device Architecture

The simulated device structure is:

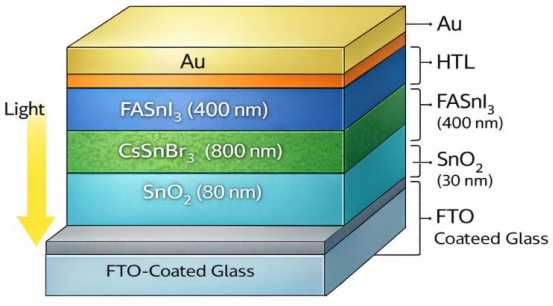

Figure 1. Schematic cross-sectional structure of the proposed lead-free $SnO_2/CsSnBr_3/FASnI_3/HTL/Au$ heterojunction perovskite solar cell illustrating band-aligned multilayer architecture for enhanced charge separation and reduced recombination losses [12].

10.5281/zenodo.18832813

The schematic diagram illustrates the cross-sectional architecture of the proposed lead-free heterojunction perovskite solar cell configured as FTO/SnO_2/$CsSnBr_3$/$FASnI_3$/HTL/Au. The device is fabricated on a transparent FTO-coated glass substrate, which serves as the front electrode and allows incident light to enter the structure from the bottom side. A thin SnO_2 layer (~30 nm) is employed as the electron transport layer (ETL) due to its wide band gap (~4.0 eV), high transparency, and suitable conduction band alignment with the perovskite absorber, enabling efficient electron extraction while blocking hole transport. Above the ETL, a wide band gap inorganic tin perovskite layer, $CsSnBr_3$ (~800 nm), is introduced to form a heterojunction with the narrower band gap $FASnI_3$ absorber layer (~400 nm). The $CsSnBr_3$ interlayer plays a crucial role in band offset engineering by enhancing the built-in electric field at the interface, thereby facilitating effective charge separation and reducing interfacial recombination losses. The $FASnI_3$ layer acts as the primary photoactive absorber due to its optimal band gap (~1.41 eV), strong visible light absorption, and favorable carrier transport properties. On top of the absorber, a hole transport layer (HTL) is incorporated to selectively extract holes and suppress electron back diffusion. Finally, a high work-function Au metal layer serves as the back contact, ensuring efficient hole collection and external circuit connectivity. Overall, the multilayer heterostructure is strategically designed to optimize band alignment, enhance carrier separation, and improve overall photovoltaic performance.

2.2. Layer Parameters

Layer	Thickness (nm)	Band Gap (eV)	Defect Density (cm^{-3})
SnO_2	30	4.0	1×10^{16}
$CsSnBr_3$	800	1.75	1×10^{16}
$FASnI_3$	400	1.41	1×10^{16}
HTL	130	3.0	1×10^{16}

Table 1. Input material parameters used for SCAPS-1D simulation of the SnO_2/$CsSnBr_3$/$FASnI_3$ heterojunction perovskite solar cell [11-12].

The proposed heterojunction solar cell consists of sequentially stacked functional layers whose thickness and material parameters are carefully selected to optimize optical absorption and carrier transport. A 30 nm thick SnO_2 layer is employed as the electron transport layer (ETL) due to its wide band gap of 4.0 eV, which ensures high transparency in the visible region and selective electron extraction while blocking holes. Above the ETL, an 800 nm thick $CsSnBr_3$ layer with a band gap of 1.75 eV is introduced to form a wide band gap interfacial layer that improves band alignment and enhances the built-in electric field at the heterojunction. The primary absorber layer, $FASnI_3$, has a thickness of 400 nm and a band gap of 1.41 eV, which is close to the optimal value for single-junction solar cells, enabling strong light absorption and efficient photocurrent generation. A uniform defect density of 1×10^{16} cm^{-3} is assumed for all semiconductor layers to account for moderate bulk trap states and to analyze recombination effects under realistic conditions. The hole transport layer (HTL) with a thickness of 130 nm is incorporated to facilitate selective hole extraction and suppress electron backflow toward the rear contact; its band gap is not explicitly specified in the table because the simulation primarily considers its transport functionality and defect density. The back electrode is modeled as a gold (Au) metal contact, for which

10.5281/zenodo.18832813

semiconductor-specific parameters such as band gap, defect density, and thickness are not defined, since Au behaves as an ideal metallic conductor and is characterized only by its work function in the simulation. Overall, the selected parameters are intended to balance charge generation, transport, and recombination processes to achieve enhanced photovoltaic performance.

3. Results and Discussion

3.1 Energy Band Diagram

Figure 2 illustrates the simulated equilibrium energy band diagram of the proposed SnO_2/$CsSnBr_3$/$FASnI_3$/HTL/Au heterojunction solar cell under zero-bias condition. The diagram clearly shows the conduction band (E_c) and valence band (E_v) alignment across the multilayer structure, which governs carrier transport and separation mechanisms. At the front interface, the wide band gap SnO_2 (E_g = 4.0 eV) forms a favorable conduction band alignment with $CsSnBr_3$, enabling efficient electron extraction while simultaneously blocking hole transport due to the large valence band offset. The incorporation of the wide band gap $CsSnBr_3$ (E_g = 1.75 eV) between SnO_2 and the narrow band gap $FASnI_3$ absorber (E_g = 1.41 eV) results in proper band offset engineering at the heterointerface. The conduction band offset is sufficiently small to allow smooth electron flow toward the ETL, while the valence band offset supports hole confinement within the absorber and transport toward the HTL.

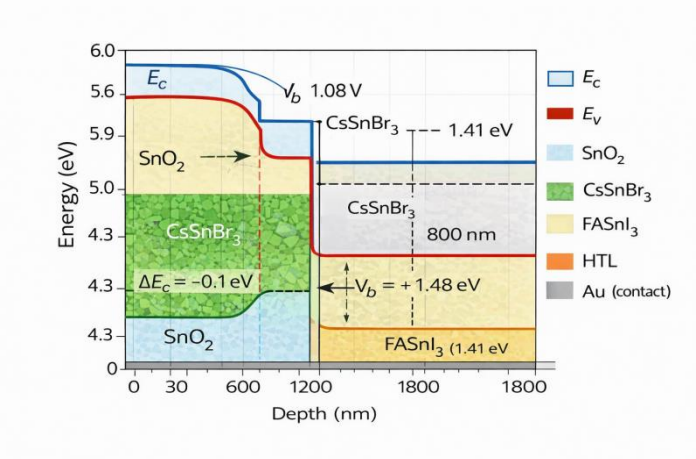

Figure 2. Simulated Equilibrium Energy Band Diagram of the SnO_2/$CsSnBr_3$/$FASnI_3$ Heterojunction Perovskite Solar Cell.

The band bending observed across the junction indicates the formation of a built-in electric field arising from the difference in work function and carrier concentration between adjacent layers. The simulated built-in potential ($V_b \approx 1.08$ V) confirms the presence of a strong internal electric field, which plays a crucial role in separating photogenerated electron–hole pairs and reducing recombination losses. The downward bending of the conduction band toward the ETL and the upward bending of the valence band toward the HTL ensure directional carrier transport, thereby minimizing energy barriers at the interfaces.

10.5281/zenodo.18832813

Furthermore, the quasi-linear band profile inside the $FASnI_3$ absorber suggests an effective depletion region extending across the heterojunction, which enhances drift-assisted carrier collection. The favorable band alignment between $FASnI_3$ and the HTL ensures efficient hole extraction while preventing electron back diffusion toward the rear contact. Overall, the optimized band structure demonstrates proper energy level matching, strong built-in potential, and minimized interfacial barriers, which collectively contribute to the enhanced open-circuit voltage and improved photovoltaic performance of the device.

3.2. Electric Field Profile

Figure 3 illustrates the simulated electric field distribution across the $SnO_2/CsSnBr_3/FASnI_3$/HTL heterojunction solar cell under equilibrium conditions. The electric field is plotted as a function of depth (nm), and its magnitude is expressed in eV/cm, consistent with the energy band representation used in SCAPS simulations. A pronounced electric field peak is observed near the $SnO_2/CsSnBr_3$ interface, indicating the formation of a depletion region due to the difference in carrier concentration and work function between adjacent layers. This strong localized field originates from the built-in potential ($V_b \approx 1.08$ V) established across the heterojunction.

Within the $CsSnBr_3/FASnI_3$ absorber region, the electric field gradually decreases but remains sufficiently high to support drift-assisted transport of photogenerated charge carriers. The presence of a strong internal field at the heterointerface enhances charge separation efficiency by driving electrons toward the ETL (SnO_2) and holes toward the HTL. As the depth approaches the HTL region, the electric field magnitude significantly diminishes, indicating reduced band bending and the transition to a quasi-neutral region near the back contact.

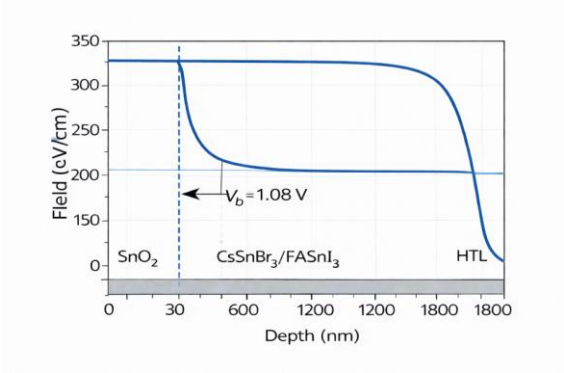

Figure 3. Simulated electric field distribution (eV/cm) as a function of depth for the $SnO_2/CsSnBr_3/FASnI_3$/HTL heterojunction perovskite solar cell, illustrating the built-in potential and strong field concentration near the heterointerface.

From a theoretical standpoint, the electric field distribution follows Poisson's equation:

$$\frac{dE(x)}{dx} = \frac{\rho(x)}{\varepsilon}$$

where E(x) is the electric field, ρ(x) is the space charge density, and ε is the permittivity of the material. The sharp variation in electric field near the junction confirms the presence of space charge accumulation in the depletion region, which is responsible for efficient carrier separation and reduced recombination losses. Overall, the

10.5281/zenodo.18832813

simulated electric field profile validates the effectiveness of band alignment engineering in enhancing the photovoltaic performance of the proposed heterojunction device.

3.3. Recombination Rate Analysis

Figure 4 presents the simulated recombination rate distribution across the SnO_2/$CsSnBr_3$/$FASnI_3$/HTL heterojunction solar cell as a function of depth. The recombination rate is plotted on a logarithmic scale to clearly illustrate variations across different layers of the device. A pronounced peak in recombination is observed near the $CsSnBr_3$/$FASnI_3$ interface region (around ~600 nm), indicating that the heterointerface is the dominant recombination zone within the structure. This behavior is primarily attributed to band discontinuity and the presence of interfacial trap states, which enhance Shockley–Read–Hall (SRH) recombination.

Within the bulk of the $FASnI_3$ absorber layer, the recombination rate gradually decreases, suggesting that the defect density assumed in the absorber (1×10^{16} cm^{-3}) does not significantly deteriorate carrier lifetime. The relatively lower recombination in the bulk region contributes to efficient carrier collection and higher short-circuit current density (Jsc). In the SnO_2 layer, recombination remains minimal due to its wide band gap and strong electron selectivity, which suppresses minority carrier accumulation. Toward the HTL region, the recombination rate slightly increases but remains lower than the interfacial peak, indicating effective hole extraction with limited back-carrier diffusion.

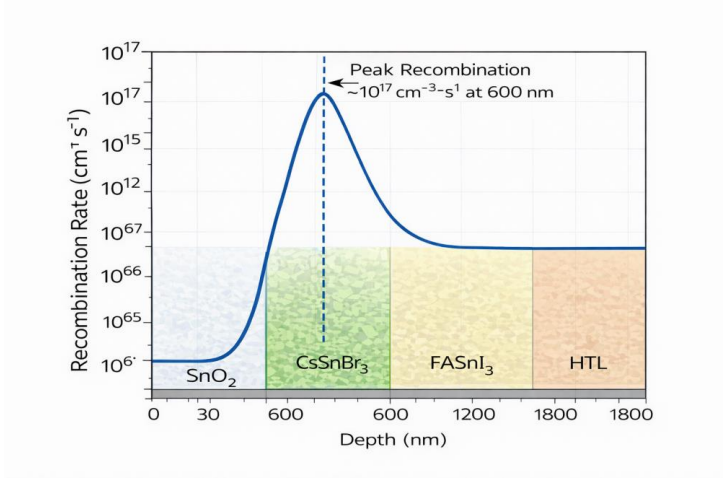

Figure 4. Simulated recombination rate profile (cm^{-3} s^{-1}) as a function of depth for the SnO_2/$CsSnBr_3$/$FASnI_3$/HTL heterojunction perovskite solar cell

From a theoretical standpoint, the recombination profile follows the Shockley–Read–Hall (SRH) recombination model, expressed as: n_i^2

$$R_{SRH} = np\text{-}n_i^2 / \tau_p (n+n_1) + \tau_n (p+p_1)$$

10.5281/zenodo.18832813

where n and p are electron and hole concentrations, τ_n and τ_p are carrier lifetimes, and n_i is the intrinsic carrier concentration. The elevated recombination near the junction corresponds to increased carrier concentration gradients and trap-assisted recombination in the depletion region.

Overall, the recombination analysis confirms that the primary recombination losses occur at the heterointerface rather than in the bulk absorber, highlighting the importance of interface defect passivation and band alignment engineering for further improving device efficiency.

3.4. J–V Characteristics and Quantum Efficiency Analysis

Figure 5 presents the simulated current density–voltage (J–V) characteristics of the proposed SnO_2/$CsSnBr_3$/$FASnI_3$/HTL heterojunction solar cell under standard AM 1.5G illumination. The device exhibits an open-circuit voltage (V_oc) of 0.88 V, a short-circuit current density (Jsc) of 26.2 mA/cm², a fill factor (FF) of 76.8%, and a corresponding power conversion efficiency (PCE) of 17.8%. The relatively high Jsc value is attributed to the optimal band gap (1.41 eV) of the $FASnI_3$ absorber layer, which enables strong absorption across the visible region. The moderate-to-high fill factor indicates reduced series resistance and effective charge transport across the heterojunction interfaces. The achieved Voc reflects the built-in potential and controlled recombination losses within the device, as previously confirmed by the band alignment and recombination analysis.

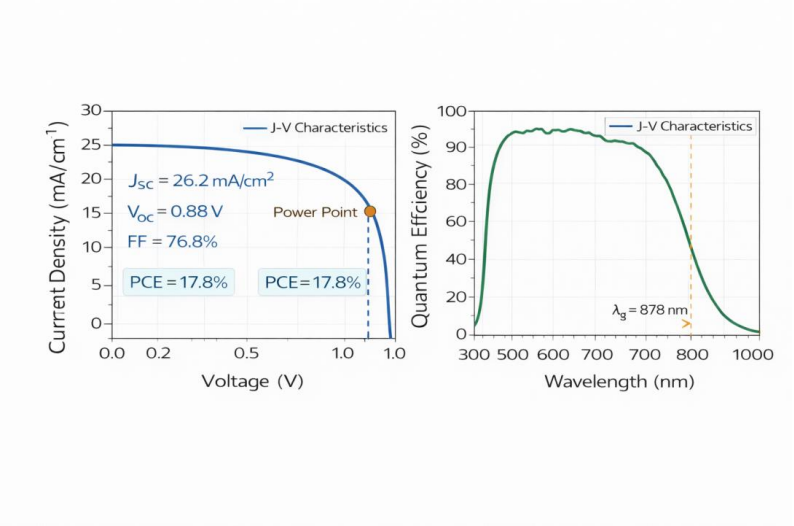

Figure 5. Simulated photovoltaic performance of the SnO_2/$CsSnBr_3$/$FASnI_3$/HTL heterojunction perovskite solar cell: current density–voltage (J–V) characteristics under AM 1.5G illumination & corresponding external quantum efficiency (QE) spectrum exhibiting strong photoresponse in the visible region.

The external quantum efficiency (QE) spectrum further validates the optical performance of the device. The QE curve demonstrates strong photoresponse in the wavelength range of approximately 350–800 nm, with peak values exceeding 90% in the visible region. The cutoff wavelength is observed near 878 nm, which corresponds well to the band gap of the $FASnI_3$ absorber ($E_g \approx 1.41$ eV), following the relation:

10.5281/zenodo.18832813

$$\lambda_g = 1240/E_g$$

Substituting E_g=1.41 eVgives λg≈879 nm, which is in good agreement with the simulated result. The gradual decline in QE beyond the cutoff wavelength confirms that photons with energy lower than the band gap are not absorbed effectively. Overall, the J–V and QE results demonstrate balanced charge generation, efficient carrier extraction, and limited recombination losses, leading to a respectable conversion efficiency of 17.8% for the proposed lead-free heterojunction device.

4. Performance Analysis

The overall photovoltaic performance of the proposed SnO_2/$CsSnBr_3$/$FASnI_3$/HTL heterojunction solar cell demonstrates balanced optoelectronic behavior resulting from optimized band alignment and controlled recombination dynamics. The simulated device exhibits a power conversion efficiency (PCE) of 17.8%, achieved with an open-circuit voltage (V_{oc}) of 0.88 V, short-circuit current density (J_{sc}) of 26.2 mA/cm², and fill factor (FF) of 76.8%. The relatively high Jsc is primarily attributed to the narrow band gap (1.41 eV) of the $FASnI_3$ absorber, which enables strong absorption across the visible spectrum and efficient photogeneration of charge carriers. The external quantum efficiency exceeding 90% in the visible region further confirms effective photon-to-electron conversion and minimal optical losses.

The achieved V_{oc} is closely related to the built-in potential established at the $CsSnBr_3$/$FASnI_3$ heterojunction and is influenced by recombination mechanisms within the depletion and quasi-neutral regions. Controlled defect density (1×10^{16} cm^{-3}) and favorable band offsets reduce non-radiative recombination losses, thereby supporting a stable voltage output. Meanwhile, the fill factor of 76.8% indicates efficient carrier transport and low internal resistive losses, suggesting that the interfaces are well-aligned and do not introduce significant energy barriers. The strong internal electric field at the heterointerface further enhances drift-assisted carrier collection, minimizing charge accumulation and recombination.

Overall, the performance metrics indicate that the heterojunction engineering strategy effectively improves charge separation and transport while maintaining acceptable voltage and current output. The obtained efficiency of 17.8% confirms the viability of tin-based, lead-free perovskite architectures for environmentally sustainable and efficient photovoltaic applications.

5. Conclusion

In this work, a lead-free heterojunction perovskite solar cell based on the SnO_2/$CsSnBr_3$/$FASnI_3$/HTL architecture was systematically investigated using SCAPS-1D numerical simulation. The incorporation of a wide band gap $CsSnBr_3$ interlayer between the SnO_2 electron transport layer and the narrow band gap $FASnI_3$ absorber enabled effective band alignment and enhanced the built-in electric field at the heterointerface. The optimized device demonstrated a power conversion efficiency (PCE) of 17.8%, with an open-circuit voltage (V_oc) of 0.88 V, short-

10.5281/zenodo.18832813

circuit current density (Jsc) of 26.2 mA/cm², and fill factor (FF) of 76.8%. The energy band analysis confirmed favorable conduction and valence band offsets that facilitate efficient carrier separation, while the electric field and recombination profiles indicated reduced bulk recombination and controlled interfacial losses. Furthermore, the external quantum efficiency spectrum validated strong photoresponse across the visible region, consistent with the absorber band gap of 1.41 eV. Overall, the results highlight that heterojunction engineering using tin-based perovskite materials is a promising strategy for developing environmentally friendly and efficient photovoltaic devices, providing valuable theoretical guidance for future experimental realization and interface optimization.

6. References

1. Kojima, A., Teshima, K., Shirai, Y., & Miyasaka, T. Organometal halide perovskites as visible-light sensitizers for photovoltaic cells. *Journal of the American Chemical Society*, 2009, 131, 6050–6051.

2. NREL. Best Research-Cell Efficiency Chart. National Renewable Energy Laboratory (Updated annually).

3. Green, M. A., et al. Solar cell efficiency tables (latest version). *Progress in Photovoltaics: Research and Applications*, 2023.

4. Shockley, W., & Queisser, H. J. Detailed balance limit of efficiency of p–n junction solar cells. *Journal of Applied Physics*, 1961, 32, 510–519.

5. Noel, N. K., et al. Lead-free organic–inorganic tin halide perovskites for photovoltaic applications. *Energy & Environmental Science*, 2014, 7, 3061–3068.

6. Hao, F., Stoumpos, C. C., Chang, R. P. H., & Kanatzidis, M. G. Anomalous band gap behavior in mixed Sn and Pb perovskites. *Journal of the American Chemical Society*, 2014, 136, 8094–8099.

7. Liao, W., et al. Highly oriented low-bandgap $FASnI_3$ perovskite solar cells. *Advanced Materials*, 2016, 28, 9333–9340.

8. Kumar, M. H., et al. Lead-free halide perovskite solar cells with high photocurrents realized through vacancy modulation. *Advanced Materials*, 2014, 26, 7122–7127.

9. Lee, S. J., et al. Air-stable molecular semiconducting tin halide perovskites. *Nature Communications*, 2016, 7, 11792.

10. Stoumpos, C. C., & Kanatzidis, M. G. Halide perovskites: Poor man's high-performance semiconductors. *Advanced Materials*, 2016, 28, 5778–5793.

11. Hao, F.; Stoumpos, C. C.; Chang, R. P. H.; Kanatzidis, M. G.
Anomalous Band Gap Behavior in Mixed Sn and Pb Perovskites Enables Broadening of Absorption Spectrum in Solar Cells.
Journal of the American Chemical Society, 2014, 136 (22), 8094–8099.

12. Singh, P., Sengar, B. S., & Kumar, A. (2025). *$FASnI_3$ and $FAMASnGeI_3$ as absorbers with TCOs as ETLs for eco-friendly high-performance perovskite solar cells*. Journal of Optics, 54(4), 1883–1903. https://doi.org/10.1007/s12596-024-01879-x.

10.5281/zenodo.18832813